Editors' Suggestion

Black Hole Solutions as Topological Thermodynamic Defects

Shao-Wen Wei,[1,2,*] Yu-Xiao Liu,[1,2,†] and Robert B. Mann[3,‡]
[1]Lanzhou Center for Theoretical Physics, Key Laboratory of Theoretical Physics of Gansu Province, School of Physical Science and Technology, Lanzhou University, Lanzhou 730000, People's Republic of China
[2]Institute of Theoretical Physics and Research Center of Gravitation, Lanzhou University, Lanzhou 730000, People's Republic of China
[3]Department of Physics and Astronomy, University of Waterloo, Waterloo, Ontario N2L 3G1, Canada

(Received 12 August 2022; accepted 10 October 2022; published 31 October 2022)

In this Letter, employing the generalized off-shell free energy, we treat black hole solutions as defects in the thermodynamic parameter space. The results show that the positive and negative winding numbers corresponding to the defects indicate the local thermodynamical stable and unstable black hole solutions, respectively. The topological number defined as the sum of the winding numbers for all the black hole branches at an arbitrary given temperature is found to be a universal number independent of the black hole parameters. Moreover, this topological number only depends on the thermodynamic asymptotic behaviors of the black hole temperature at small and large black hole limits. Different black hole systems are characterized by three classes via this topological number. This number could help us in better understanding the black hole thermodynamics and, further, shed new light on the fundamental nature of quantum gravity.

DOI: 10.1103/PhysRevLett.129.191101

Introduction.—Black holes predicted by general relativity play a central role in modern physics. Observations of binary black hole mergers by the LIGO/Virgo Collaboration [1] and reconstruction of event-horizon-scale images of M87* by the Event Horizon Telescope [2] have opened new windows to study the strong gravitational nature of black holes. Alternatively, seeking underlying characteristic properties of black holes is also quite valuable, since they can yield features that can be tested by further astronomical observations.

One such approach is topology: by ignoring detailed structure, generic properties of a system can be discerned. This approach has been extensively employed to study many physical phenomena such as magnetic monopoles, the quantum Hall effect, and superconductivity. A key concept is that of defects, which are generally thought to be related to zero points of a field at $\vec{x}=\vec{z}$,

$$\phi(\vec{x})|_{\vec{x}=\vec{z}}=0, \tag{1}$$

in a space, and which can reveal certain properties of field configurations. In different dimensions, a defect can be a point charge, a string, or even a domain wall. The most simple topological quantity associated with the zero point of a field is its winding number. When equipped with it, we can determine the nature of a system possessing defects.

Of particular recent interest has been a special vector constructed in the coordinate space of a black hole spacetime [3,4] by making use of null geodesics. The light ring of a black hole is located exactly at the zero point of this vector field. After calculating the winding number corresponding to this zero point, a four-dimensional stationary nonextremal spinning black hole in asymptotically flat spacetime with a topologically spherical Killing horizon was shown to allow at least one standard light ring outside the horizon for each sense of rotation [4]. This treatment was generalized to other cases, where the critical points and timelike circular orbit were well studied [5–11].

In general relativity, a black hole solution satisfies the Einstein field equations, which we reformulate as

$$\mathcal{E}_{\mu\nu}\equiv G_{\mu\nu}-\frac{8\pi G}{c^4}T_{\mu\nu}=0. \tag{2}$$

We propose, analogous to Eq. (1), that a physical black hole solution is a zero point of the tensor field $\mathcal{E}_{\mu\nu}$, at which all its components vanish. Although the Einstein field equations also admit other defectlike solutions, such as cosmic strings and branes, we here only focus on black holes. As a result, we can endow a black hole solution with a topological charge as well. Adopting this topological argument, we can then study the local and global particular properties of a black hole. Different black hole solutions are also expected to be divided into different classes.

Realization in thermodynamics.—As a starting point to realize the idea that a black hole solution possesses a topological charge, we begin with black hole thermodynamics.

In 1977, Gibbons and Hawking [12] proposed that the partition function of a canonical ensemble for black holes can be evaluated with its Euclidean action in the form of the

gravitational path integral. In the "zero-loop" approximation, it reads

$$\mathcal{Z} = e^{-\beta F} = \int D[g] e^{-\frac{\mathcal{I}}{\hbar}} \sim e^{-\frac{\mathcal{I}}{\hbar}}, \tag{3}$$

where F and $\mathcal{I}$ are the free energy and Euclidean action of the black hole. The period β of the Euclidean time is the inverse of the black hole temperature. Following this approach, it was found that negative heat capacity and imaginary energy fluctuations were produced. Soon afterward, these shortcomings were solved by York [13] by imagining that the black hole is placed inside a cavity. Fixing the temperature T of the cavity surface, the results show that the heavy-mass black hole branch with mass $M > \sqrt{3}/8\pi T$ is thermodynamically stable, and thus the corresponding partition function is well-defined.

In order to describe a black hole with an arbitrary mass, York defined a generalized free energy following the standard definition of the free energy with the mass and temperature being two independent variables [13]. This naturally extends one more dimension for the thermodynamic parameter space of the black hole. Furthermore, the generalized free energy reduces to the standard one when the relation between the black hole mass and temperature is satisfied [14].

Inspired by this, we would like to introduce the generalized free energy

$$\mathcal{F} = E - \frac{S}{\tau} \tag{4}$$

for a black hole system with energy E and entropy S. The parameter τ is an extra variable having the dimension of time, and can be thought as the inverse temperature of the cavity enclosing the black hole. Here, we let the time parameter τ vary freely instead of the mass [13]. In general this generalized free energy is off-shell except at

$$\tau = T^{-1}, \tag{5}$$

at which the black hole solution satisfies the Einstein field equations [Eq. (2)]. Recently, a similar generalized free energy [Eq. (4)] has been used to study the dynamic evolution of black hole phase transitions [15–18].

We now describe the explicit construction for the vector ϕ in Eq. (1) via a thermodynamic approach. We define

$$\phi = \left(\frac{\partial \mathcal{F}}{\partial r_{\mathrm{h}}}, -\cot\Theta \csc\Theta \right), \tag{6}$$

where, inspired by the axis limit [4], we introduce a parameter $0 \le \Theta \le \pi$ for convenience. At $\Theta = 0, \pi$, the component ϕ^{Θ} diverges and thus the direction of the vector is outward.

More importantly, the zero points of ϕ correspond to the conditions $\Theta = \pi/2$ and $\tau = T^{-1}$. This confirms that the black hole solution exactly meets the zero point of the vector ϕ. Therefore, from the viewpoint of topology, we can endow each black hole solution with a topological charge by using ϕ.

Following Duan's ϕ-mapping topological current theory [19,20], we can introduce the topological current as

$$j^{\mu} = \frac{1}{2\pi} \epsilon^{\mu\nu\rho} \epsilon_{ab} \partial_{\nu} n^{a} \partial_{\rho} n^{b}, \qquad \mu, \nu, \rho = 0, 1, 2, \tag{7}$$

where $\partial_{\nu} = (\partial/\partial x^{\nu})$ and $x^{\nu} = (\tau, r_h, \Theta)$. The unit vector is defined as $n^{a} = (\phi^{a}/\|\phi\|)$ $(a = 1, 2)$ with $\phi^{1} = \phi^{r_h}$ and $\phi^{2} = \phi^{\Theta}$. Here, the parameter τ can be considered as a time parameter of the topological defect. Moreover, it is easy to check that this topological current is conserved, i.e., $\partial_{\mu} j^{\mu} = 0$. By making use of the Jacobi tensor $\epsilon^{ab} J^{\mu}(\phi/x) = \epsilon^{\mu\nu\rho} \partial_{\nu} \phi^{a} \partial_{\rho} \phi^{b}$ and the two-dimensional Laplacian Green function $\Delta_{\phi^a} \ln \|\phi\| = 2\pi \delta^{2}(\phi)$, the topological current can be reexpressed as [5]

$$j^{\mu} = \delta^{2}(\phi) J^{\mu}\left(\frac{\phi}{x}\right). \tag{8}$$

Obviously, j^{μ} is nonzero only at $\phi^{a}(x^{i}) = 0$, and we denote its ith solution as $\vec{x} = \vec{z}_i$. The density of the topological current is then [21]

$$j^{0} = \sum_{i=1}^{N} \beta_i \eta_i \delta^{2}(\vec{x} - \vec{z}_i). \tag{9}$$

The positive Hopf index β_i counts the number of the loops that ϕ^{a} makes in the vector ϕ space when x^{μ} goes around the zero point z_i, and the Brouwer degree $\eta_i = \mathrm{sign}(J^{0}(\phi/x)_{z_i}) = \pm 1$. Given a parameter region Σ, the corresponding topological number can be obtained

$$W = \int_{\Sigma} j^{0} d^{2}x = \sum_{i=1}^{N} \beta_i \eta_i = \sum_{i=1}^{N} w_i, \tag{10}$$

where w_i is the winding number for the ith zero point of ϕ contained in Σ. If two given loops $\partial\Sigma$ and $\partial\Sigma'$ enclose the same zero point of ϕ, they possess the same winding number. Alternatively, if there is no zero point in the enclosed region, we will have $W = 0$. If Σ is the neighborhood of a zero point of ϕ, it will yield local topological properties, whereas if Σ is the entire parameter space, the global topological W number will be revealed.

In the above approach, the isolated zero points require the Jacobian $J_0(\phi/x) \neq 0$. If this condition is violated, the defect bifurcates [22].

Local and global topological properties.—Following Eq. (3), one can obtain the free energy by calculating the first-order Euclidean Einstein action

$$\mathcal{I} = -\frac{1}{16\pi} \int \sqrt{g} R d^{4}x + \frac{1}{8\pi} \oint \sqrt{\gamma} K d^{3}x - \mathcal{I}_{\mathrm{subtract}}, \tag{11}$$

where K is the trace of the extrinsic curvature, γ_{ij} is the induced metric on the boundary, and $\mathcal{I}_{\mathrm{subtract}}$ is the subtraction term.

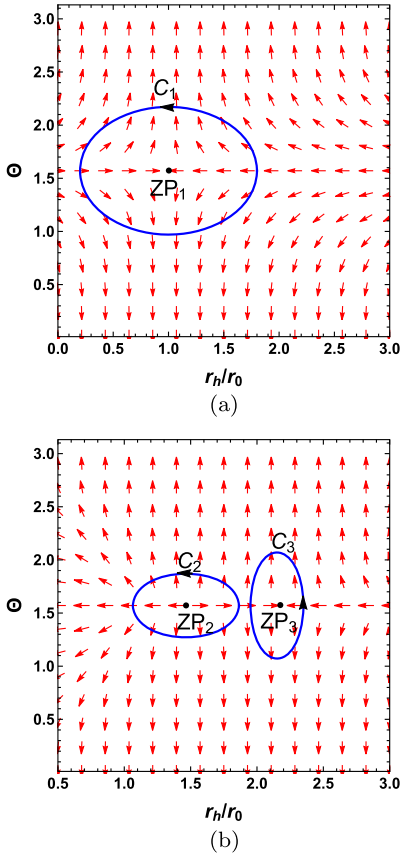

FIG. 1. The red arrows represent the unit vector field n on a portion of the r_h-Θ plane. The zero points (ZPs) marked with black dots are at $(r_h/r_0, \Theta) = (1, (\pi/2))$, (1.46, $(\pi/2)$), and (2.15, $(\pi/2)$), for ZP_1, ZP_2, and ZP_3, respectively. The blue contours C_i are closed loops enclosing the zero points. (a) The unit vector field for the Schwarzschild black hole with $\tau/r_0 = 4\pi$. (b) The unit vector field for the RN black hole with $\tau/r_0 = 34.48$ and $Q/r_0 = 1$.

For the Schwarzschild black hole, one easily has $E = \partial_\beta \mathcal{I} = M$ and $S = (\beta\partial_\beta \mathcal{I} - \mathcal{I}) = 4\pi M^2$ [12]. Accordingly, the black hole thermodynamic relations can be deduced straightforwardly. For the Schwarzschild black hole, we obtain the generalized free energy $\mathcal{F} = (r_h/2) - (\pi r_h^2/\tau)$, where $r_h = 2M$. Then the components of the constructed vector ϕ can be calculated

$$\phi^{r_h} = \frac{1}{2} - \frac{2\pi r_h}{\tau}, \tag{12}$$

$$\phi^{\Theta} = -\cot\Theta \csc\Theta. \tag{13}$$

We show the unit vector field n on a portion of the Θ-r_h plane in Fig. 1(a) for the Schwarzschild black hole with $\tau = 4\pi r_0$ with r_0 an arbitrary length scale set by the size of a cavity surrounding the black hole.

From the figure, the zero point is located at $r_h/r_0 = 1$ and $\Theta = \pi/2$. Since the winding number w is independent of these loops enclosing the zero point, we can calculate it for an arbitrary loop; for example see C_1 given in Fig. 1(a). Performing the calculation, we obtain the winding number $w = -1$. If we choose an alternate orientation convention by adding a minus sign in ϕ^{r_h} in Eq. (6), we obtain $w = 1$ instead. However, the winding numbers of other types of black holes will likewise be changed.

Considering the gravitational action together with the electromagnetic field, it is easy to find $E = (r_h^2 + Q^2)/2r_h$ and $S = \pi r_h^2$ for the Reissner-Nordström (RN) black hole. Thus, the generalized free energy is

$$\mathcal{F} = \frac{r_h^2 + Q^2}{2r_h} - \frac{\pi r_h^2}{\tau}. \tag{14}$$

Here, τ can be thought as the inverse temperature of the cavity. Thus r_h is independent of τ, and can vary freely, ignoring the lower bound. Employing it, we plot the unit vector field n in Fig. 1(b) for arbitrarily chosen typical values $\tau/r_0 = 34.48$ and $Q/r_0 = 1$.

We find two zero points, ZP_2 and ZP_3, at $r_h/r_0 = 1.46$ and 2.15, respectively. A detailed calculation shows that their respective winding numbers are $w = 1$ and -1. We also obtain the heat capacities $C_Q/r_0^2 = 18.01$ and -64.81 at constant charge $Q/r_0 = 1$ for the respective positive and negative zero points. Noting that each zero point of the unit vector has a winding number 1 or -1, from this we conjecture that winding number is related to local thermodynamic stability, with positive and negative values corresponding to stable and unstable black hole solutions.

Turning to global properties of the topology, if we choose the region Σ as the whole parameter space or the loop $\partial\Sigma$ as the boundary of the parameter space, i.e., $(0 < \Theta < \pi) \cup (0 < r_h < \infty)$, we can obtain the topological number W for a black hole solution. This global property can be used to classify different black hole solutions. Since we here take the axis limit, where the direction of the vector ϕ is up at $\Theta = \pi$ and down at $\Theta = 0$, the value of the topological number W actually depends on the direction of the vector at $r_h = 0$ and ∞. This suggests that black hole solutions sharing the same behavior at $r_h = 0$ and ∞ possess the same topological number, and thus are topologically equivalent.

By solving the equation $\phi^{r_h} = 0$, we can obtain a curve in the r_h-τ plane. The results are

$$\tau = 4\pi r_h \tag{15}$$

and

$$\tau = \frac{4\pi r_h^3}{r_h^2 - Q^2} \tag{16}$$

for the Schwarzschild and RN black holes, respectively. To show zero points of the component ϕ^{r_h}, we plot these two curves in Fig. 2. For large τ (e.g., $\tau = \tau_2$) there are

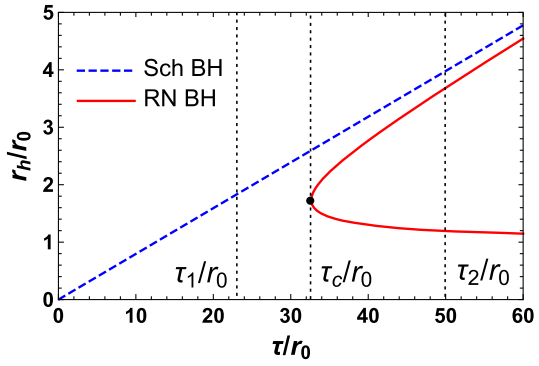

FIG. 2. Zero points of the vector ϕ shown in the r_h-τ plane. The blue dashed and red solid lines are for the Schwarzschild black hole (Sch BH) and RN black hole (RN BH) with $Q/r_0 = 1$. The black dot with $\tau_c = 6\sqrt{3}\pi Q$ denotes the generation point for the RN black hole. At $\tau = \tau_1$, there is one Schwarzschild black hole, and at $\tau = \tau_2$, there is one Schwarzschild black hole and two RN black holes.

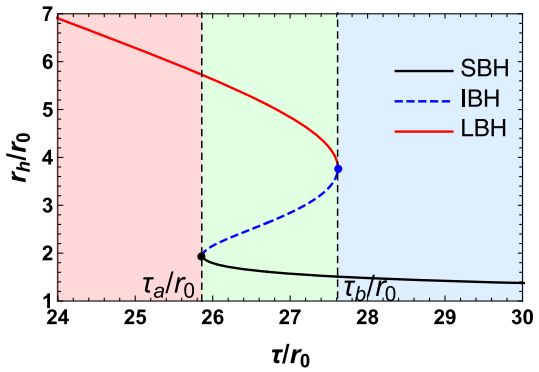

FIG. 3. Zero points of ϕ^{r_h} shown in the r_h-τ plane for the RN-AdS black hole with $Pr_0^2 = 0.0022$ and $Q/r_0 = 1$. The black solid, blue dashed, and red solid lines are for the small black hole (SBH), intermediate black hole (IBH), and large black hole (LBH), respectively. Black and blue dots are the annihilation and generation points. Different color regions have different numbers of the black hole branches. However, their W number is constant and equals 1.

respectively one and two intersection points for the Schwarzschild and RN black holes. The intersection points exactly satisfy the condition Eq. (5), and therefore denote the on-shell black hole solutions with temperature $T = \tau^{-1}$. In contrast to the Schwarzschild black hole, for $\tau < \tau_c$, the two intersection points for the RN black hole coincide and then disappear. Based on the local property of a zero point, we have the topological number $W = -1$ for the Schwarzschild black hole, while $W = 1 - 1 = 0$ for the RN black hole with the charge $Q/r_0 = 1$. In particular, at the point $\tau_c = 6\sqrt{3}\pi Q$, it is easy to get $(d^2\tau/dr_h^2) = 6\sqrt{3}\pi/Q > 0$ for the RN black hole. This suggests that τ_c is a generation point, which can also be observed in Fig. 2.

To investigate whether or not W depends on the charge, we examine the behavior of the curve $\tau(r_h)$ in Eq. (16) at the limit $r_h \to r_E = Q$ (corresponding to extremal RN black hole with smallest horizon) and ∞. Obviously, for a nonvanishing charge Q, the vanishing or diverging behavior of τ as $r_h \to r_E/\infty$ does not change, and so W remains the same for different values of Q. For the Schwarzschild black hole with $Q = 0$, the behavior of $\tau(r_h)$ for small r_h differs from the charged case, and so the topological numbers W for the two black hole solutions are different.

Another interesting black hole solution is the charged Reissner-Nordström anti–de Sitter (RN-AdS) black hole, which exhibits a small-large black hole phase transition [23]. In the extended phase space, the cosmological constant is treated as the pressure P of the system [24]. The free energy is

$$\mathcal{F} = \frac{8\pi P r_h^4 + 3r_h^2 + 3Q^2}{6r_h} - \frac{\pi r_h^2}{\tau}. \tag{17}$$

Taking the pressure $Pr_0^2 = 0.0022$ to be smaller than its critical value, we exhibit zero points of ϕ^{r_h} in the r_h-τ plane in Fig. 3 with $Q/r_0 = 1$. Quite different from the Schwarzschild and RN black holes shown in Fig. 2, we observe that there are three black hole branches for $\tau_a < \tau < \tau_b$, one small black hole branch for $\tau < \tau_a$, and one large black hole branch for $\tau > \tau_b$. Computing the winding number for these black hole branches, we find that the small and large black hole branches have $w = 1$, while the intermediate black hole branch has $w = -1$. Therefore, at this pressure the RN-AdS black hole always has $W = 1 - 1 + 1 = 1$, which is independent of τ. Since the pressure P is positive for the RN-AdS black hole, it does not affect the asymptotic behavior of τ at small and large r_h. As a result, the topological number W is always unity for the RN-AdS black hole. Furthermore, our result that thermodynamically stable small and large black holes have $w = 1$ and unstable intermediate black holes have $w = -1$ supports our conjecture that a positive or negative winding number is indicative of thermodynamic stability or instability.

Note that for these values of Pr_0^2 and Q/r_0, one generation point and one annihilation point can be found at $\tau/r_0 = \tau_a/r_0 = 25.84$ and $\tau/r_0 = \tau_b/r_0 = 27.62$,

TABLE I. The topological number W, numbers of annihilation, and generation points for the Schwarzschild, RN, and RN-AdS black holes.

	Sch BH	RN BH	RN-AdS BH
W	-1	0	1
Generation point	0	1	1 or 0
Annihilation point	0	0	1 or 0

respectively. If the pressure is larger than its critical value, r_h/r_0 will be a monotonically increasing function of τ/r_0, and thus no bifurcation phenomenon will be observed. However, the topological number W still stays the same.

In the Supplemental Material [25], we show that d-dimensional RN-AdS black holes also have topological number $W = 1$, consistent with the $d = 4$ case [25].

Conclusions.—Summarizing our results in Table I, we have constructed a universal topological number W by treating the black hole solution as a defect from the viewpoint of thermodynamics. Different black hole solutions are characterized by different topological numbers and belong to different topological classes.

Locally, each zero point of the vector field defined in Eq. (6) with the generalized free energy exactly corresponds to one on-shell black hole solution. Thus, each black hole solution is endowed with one winding number. Our study shows that the thermodynamic stability of the black hole is indicated from the value of the winding number. A positive or negative winding number corresponds to thermodynamically stable or unstable black hole solutions. Of particular interest are the annihilation and generation points, which may be quite important for the time evolution of a black hole placed in a cavity.

When considering the full parameter space, the topological number W provides us with a global topological property of a black hole solution. We have shown that the Schwarzschild black hole, RN black hole, and RN-AdS black hole have, respectively, $W = -1$, 0, and 1, independent of the black hole parameters. Since the topological number W is the sum of the winding numbers for the zero points of the vector, and it is only dependent on the behavior of the curve $\tau(r_h)$ at small and large r_h limits, we conjectured that the topological number W can take three values: -1, 0, and 1. This suggests that other black hole solutions shall be divided into three characteristic topological classes, a conjecture in need of further confirmation.

We close by considering whether geometric modifications to black holes, such as those induced by scalar hair, affect the topological number W. In contrast to global charges (primary hair), black holes possessing new nontrivial fields (secondary or pseudo hair) have long been of interest in string theory [29–31] and have attracted much recent attention in both general relativity and modified gravity theories [27,28,32–37]. For the Einstein-Maxwell scalar model [27,28], we show in the Supplemental Material [25] that the topological number $W = 0$ for these scalarized black holes, the same as that of the RN black holes, and in support of the expectation that secondary (scalar) hair does not change W despite the fact that it modifies the free energy of a black hole [25]. In more general string-theoretic settings (for example axion fields with Lorentz Chern-Simons coupling to gravity [29]), the generalized free energy will be modified. Investigation of the topological charge for these more general black holes with hair is an interesting project for further study.

In conclusion, our topological approach classifies each black hole solution into certain classes sharing the similar thermodynamic properties. It provides a considerable material for the topology of black hole thermodynamics. We expect to uncover the deeper nature of other black hole solutions via the topological approach.

This work was supported by the National Natural Science Foundation of China (Grants No. 12075103, No. 11875151, and No. 12047501), the 111 Project (Grant No. B20063), and the National Key Research and Development Program of China (Grant No. 2020YFC2201503) and by the Natural Sciences and Engineering Research Council of Canada.

*Corresponding author.
weishw@lzu.edu.cn
†Corresponding author.
liuyx@lzu.edu.cn
‡Corresponding author.
rbmann@uwaterloo.ca

[1] B. P. Abbott *et al.* (Virgo, LIGO Scientific Collaborations), Observation of Gravitational Waves from a Binary Black Hole Merger, Phys. Rev. Lett. **116**, 061102 (2016).
[2] K. Akiyama *et al.* (Event Horizon Telescope Collaboration), First M87 Event Horizon Telescope results. I. The shadow of the supermassive black hole, Astrophys. J. **875**, L1 (2019).
[3] P. V. P. Cunha, E. Berti, and C. A. R. Herdeiro, Light Ring Stability in Ultra-Compact Objects, Phys. Rev. Lett. **119**, 251102 (2017).
[4] P. V. P. Cunha and C. A. R. Herdeiro, Stationary Black Holes and Light Rings, Phys. Rev. Lett. **124**, 181101 (2020).
[5] S.-W. Wei, Topological charge and black hole photon spheres, Phys. Rev. D **102**, 064039 (2020).
[6] M. Guo and S. Gao, Universal properties of light rings for stationary axisymmetric spacetimes, Phys. Rev. D **103**, 104031 (2021).
[7] S.-W. Wei and Y.-X. Liu, Topology of black hole thermodynamics, Phys. Rev. D **105**, 104003 (2022).
[8] M. B. Ahmed, D. Kubiznak, and R. B. Mann, Vortex/anti-vortex pair creation in black hole thermodynamics, arXiv:2207.02147.
[9] P. K. Yerra and C. Bhamidipati, Topology of black hole thermodynamics in Gauss-Bonnet gravity, Phys. Rev. D **105**, 104053 (2022).
[10] P. K. Yerra and C. Bhamidipati, Topology of Born-Infeld AdS black holes in 4D novel Einstein-Gauss-Bonnet gravity, arXiv:2207.10612.
[11] S.-W. Wei and Y.-X. Liu, Topology of equatorial timelike circular orbits around stationary black holes, arXiv:2207.08397.
[12] G. W. Gibbons and S. W. Hawking, Action integrals and partition functions in quantum gravity, Phys. Rev. D **15**, 2752 (1977).

[13] J. W. York, Black-hole thermodynamics and the Euclidean Einstein action, Phys. Rev. D **33**, 2092 (1986).
[14] B. F. Whiting, Black holes and gravitational thermodynamics, Classical Quantum Gravity **7**, 15 (1990).
[15] R. Li and J. Wang, Thermodynamics and kinetics of Hawking-Page phase transition, Phys. Rev. D **102**, 024085 (2020).
[16] R. Li, K. Zhang, and J. Wang, Thermal dynamic phase transition of Reissner-Nordstrom Anti-de Sitter black holes on free energy landscape, J. High Energy Phys. 10 (2020) 090.
[17] S.-W. Wei, Y.-Q. Wang, and Y.-X. Liu, Dynamic properties of thermodynamic phase transition for five-dimensional neutral Gauss-Bonnet AdS black hole on free energy landscape, Nucl. Phys. **B976**, 115692 (2022).
[18] S.-W. Wei, Y.-Q. Wang, Y.-X. Liu, and R. B. Mann, Observing dynamic oscillatory behavior of triple points among black hole thermodynamic phase transitions, Sci. China Phys. Mech. Astron. **64**, 270411 (2021).
[19] Y. S. Duan and M. L. Ge, *SU* (2) gauge theory and electrodynamics of *N* moving magnetic monopoles, Sci. Sin. **9**, 1072 (1979).
[20] Y. S. Duan, The structure of the topological current, Report No. SLAC-PUB-3301, 1984.
[21] J. A. Schouton, *Tensor Analysis for Physicists* (Claredon, Oxford, 1951).
[22] L.-B. Fu, Y.-S. Duan, and H. Zhang, Evolution of the Chern-Simons vortices, Phys. Rev. D **61**, 045004 (2000).
[23] D. Kubiznak and R. B. Mann, *P-V* criticality of charged AdS black holes, J. High Energy Phys. 07 (2012) 033.
[24] D. Kastor, S. Ray, and J. Traschen, Enthalpy and the mechanics of AdS black holes, Classical Quantum Gravity **26**, 195011 (2009).
[25] See Supplemental Material, which includes Refs. [26–28], at http://link.aps.org/supplemental/10.1103/PhysRevLett.129.191101 for the study of higher dimensional charged AdS black holes and the study of scalarized black holes.
[26] A. Chamblin, R. Emparan, C. V. Johnson, and R. C. Myers, Charged AdS black holes and catastrophic holography, Phys. Rev. D **60**, 064018 (1999).
[27] C. A. R. Herdeiro, E. Radu, N. Sanchis-Gual, and J. A. Font, Spontaneous Scalarisation of Charged Black Holes, Phys. Rev. Lett. **121**, 101102 (2018).
[28] R. A. Konoplya and A. Zhidenko, Analytical representation for metrics of scalarized Einstein-Maxwell black holes and their shadows, Phys. Rev. D **100**, 044015 (2019).
[29] B. A. Campbell, M. J. Duncan, N. Kaloper, and K. A. Olive, Axion hair for Kerr black holes, Phys. Lett. B **251**, 34 (1990).
[30] B. A. Campbell, N. Kaloper, and K. A. Olive, Classical hair for Kerr-Newman black holes in string gravity, Phys. Lett. B **285**, 199 (1992).
[31] P. Kanti, N. E. Mavromatos, J. Rizos, K. Tamvakis, and E. Winstanley, Dilatonic black holes in higher curvature string gravity, Phys. Rev. D **54**, 5049 (1996).
[32] C. A. R. Herdeiro and E. Radu, Kerr Black Holes with Scalar Hair, Phys. Rev. Lett. **112**, 221101 (2014).
[33] C. A. R. Herdeiro and E. Radu, Asymptotically flat black holes with scalar hair: A review, Int. J. Mod. Phys. D **24**, 1542014 (2015).
[34] H. O. Silva, J. Sakstein, L. Gualtieri, T. P. Sotiriou, and E. Berti, Spontaneous Scalarization of Black Holes and Compact Stars from a Gauss-Bonnet Coupling, Phys. Rev. Lett. **120**, 131104 (2018).
[35] P. V. P. Cunha, C. A. R. Herdeiro, and E. Radu, Spontaneously Scalarised Kerr Black Holes, Phys. Rev. Lett. **123**, 011101 (2019).
[36] E. Berti, L. G. Collodel, B. Kleihaus, and J. Kunz, Spin-Induced Black Hole Scalarization in Einstein-Scalar-Gauss-Bonnet Theory, Phys. Rev. Lett. **126**, 011104 (2021).
[37] C.-Y. Zhang, Q. Chen, Y. Liu, W.-K. Luo, Y. Tian, and B. Wang, Critical Phenomena in Dynamical Scalarization of Charged Black Hole, Phys. Rev. Lett. **128**, 161105 (2022).